Thermodynamic Limits of Photon-Multiplier Luminescent Solar Concentrators

Tomi K. Baikie⬤, Arjun Ashoka, Akshay Rao, and Neil C. Greenham⬤[*]

Cavendish Laboratory, University of Cambridge, Cambridge, CB3 0HE, United Kingdom

Luminescent solar concentrators (LSCs) are theoretically able to concentrate both direct and diffuse solar radiation with extremely high efficiencies. Photon-multiplier luminescent solar concentrators (PM-LSCs) contain chromophores that exceed 100% photoluminescence quantum efficiency. PM-LSCs have recently been experimentally demonstrated and hold promise to outcompete traditional LSCs. However, we find that the thermodynamic limits of PM-LSCs are different and are sometimes more extreme relative to traditional LSCs. As might be expected, to achieve very high concentration factors, a PM-LSC design must also include a free energy change, analogous to the Stokes shift in traditional LSCs. Notably, unlike LSCs, the maximum concentration ratio of a PM-LSC is dependent on the brightness of the incident photon field. For some brightnesses, but equivalent energy loss, the PM-LSC has a greater maximum concentration factor than that of the traditional LSC. We find that the thermodynamic requirements to achieve highly concentrating PM-LSCs differ from those of traditional LSCs. The new model gives insight into the limits of concentration of PM-LSCs and may be used to extract design rules for further PM-LSC design.

I. INTRODUCTION

There is currently much interest in improving the yield of solar energy capture technologies, by making better use of the incoming solar radiation. One way to improve the solar cell effectiveness is to concentrate incoming solar irradiation [1–3]. But in many regions of the world, the majority of the incident light is diffuse, but diffuse light cannot be concentrated by traditional image-preserving optical techniques, due to the limits established by the second law of thermodynamics [4,5]. Traditional luminescent solar concentrators (LSC) offer an elegant way around this problem. An LSC is typically constructed from plastic or glass sheets with embedded chromophores, organic dyes, or semiconductor nanocrystals, which efficiently absorb and emit light (Fig. 1). There is typically a free energy change that offsets the entropic loss when concentrating diffuse light. The LSC can thus concentrate both direct and diffuse light.

In traditional LSCs, a high-energy absorbed photon is converted into a lower-energy photon by the absorption and emission of a chromophore, inducing thermal loss in the form of a Stokes shift. The thermodynamics

and efficiency limits of these systems have been previously described in detail [1,6,7]. Recently, there have been proposals and experimental demonstrations of a new class of photon-multiplier luminescent solar concentrators (PM-LSC), where high-energy photons are converted into two low-energy photons via processes such as quantum cutting in lanthanide-doped nanocrystals. Chromophores exhibiting up to 180% photoluminescence quantum efficiency (PLQE) have been experimentally demonstrated [8,9]. Such systems could enable PLQEs as high as 200%. The low reabsorption and high PLQEs could make such systems ideal candidates for LSCs. There is currently no theoretical treatment of the thermodynamic limits of such a system, which is often useful to benchmark real device efficiencies against [10].

Here, we present a revised thermodynamic model, following the methods presented by Yablonovitch, which gives insight into the fundamental limits of PM-LSCs [1]. The maximum concentration performance of PM-LSCs is linked to the brightness of the incoming photon field, which is not the case for traditional LSCs. Furthermore, the maximum concentration factors associated with PM-LSCs are different and at high brightness are more extreme, relative to their traditional counterparts.

II. ETENDUE AND ENTROPY

A beam of radiation, passing through an absorbing and luminescent medium, can be characterized by a temperature, chemical potential, and etendue [11,12]. For a beam
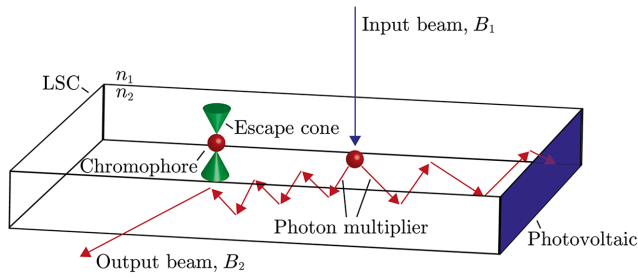
*ncg11@cam.ac.uk

FIG. 1. Schematic of operation of a photon-multiplier luminescent solar concentrator (PM-LSC). As an input beam, B_1, irradiates the device, a chromophore absorbs and emits light at a longer wavelength. In a PM-LSC, maximally two photons are emitted for every incoming photon. Supposing isotropic emission, the number of photons lost through the escape cone is dependent on the ratio of the refractive indices of the outside medium (n_1) to the medium of the LSC (n_2). Photons that are emitted within the LSC are described by the second concentrated beam, B_2, which, during proper operation, impinges on a photovoltaic mounted on the edge of the LSC.

with a ray direction within solid angle $d\Omega$, passing through an area dA, the element of etendue, $d\xi$, is given by

$$d\xi = n^2 \cos(\theta) d\Omega \, dA, \tag{1}$$

where θ is the angle between the direction of propagation and the normal to dA, and n is the refractive index of the medium. The etendue of a beam propagating through a clear and transparent medium is conserved. This conservation of etendue can be interpreted as the Liouville theorem of classical mechanics, applied to photon propagation along rays in geometrical optics. Should absorption and remission occur, the etendue change is then a measure of the free energy loss. At moderate intensities of light, the thermodynamics of the system can be described by a two-dimensional gas, where the number of dimensions arises from the two angular coordinates required to specify the direction of the beam [13].

Notably, if entropy and etendue are constant, any concentration system that decreases the illuminated area, A, must increase the angular divergence of the beam. In the case of diffuse light, the angular divergence is already maximal, and thus, diffuse radiation cannot be concentrated with a system using only geometrical optics. In a traditional LSC, the change in enthalpy from heat dissipation associated with the Stokes shift can offset the entropic loss, allowing for the concentration of diffuse light with an associated energetic penalty.

The Heisenberg uncertainty principle, considered in the absence of diffraction, places a limit on the spread of the beam wavevectors in momentum space, $dx \, dp_x \geq h$ [12]. This condition naturally requires that only a single quantum state occupies the phase-space volume,

$dx \, dy \, dz \, dp_x \, dp_y \, dp_z$. A suitable choice of coordinate system gives the beam area, dA, as $dx \, dy$. The etendue element can then be written as

$$d\xi = \frac{n^2}{k^2} dx \, dy \, dk_x \, dk_y. \tag{2}$$

The volume element $dx \, dy \, dk_x \, dk_y$ in the phase space of variables x, y, k_x, k_y is equal to $k^2 d\xi / n^2$, where n is the refractive index, and contains a single quantum state that can be occupied by a photon in a beam. For a system of N photons, and allowing for two directions of polarization, we define

$$G = \frac{2k^2}{n^2} \xi = \frac{2v^2}{c^2} \xi, \tag{3}$$

which can be interpreted as the number of quantum states within a beam with frequency $v = ck/n$ and etendue ξ. These N indistinguishable photons are distributed over the G states according to

$$W = \frac{(G+N)!}{G!N!} \approx \frac{(G+N)^{G+N}}{G^G N^N}, \tag{4}$$

where the Stirling approximation is used to obtain the second result. Invoking the ergodic hypothesis that each microstate is equally probable, the entropy of the beam, S, is the natural logarithm of the number of microstates, W, multiplied by the Boltzmann constant, k_B,

$$S = k_B \ln(W),$$
$$= k_B \frac{2v^2}{c^2} \xi \left(\left(1 + \frac{N}{G} \right) \ln \left(1 + \frac{N}{G} \right) - \frac{N}{G} \ln \left(\frac{N}{G} \right) \right). \tag{5}$$

Following Yablonovitch's treatment, the entropy per photon, s, is the number differential of the entropy of the beam [1]:

$$s = \frac{dS}{dN} = k_B \ln \left(1 + \frac{2v^2}{c^2} \frac{\xi}{N} \right). \tag{6}$$

In the limit of maximum efficiency, where the loss of one photon from the incoming beam immediately results in the addition of two photons to the concentrated beam, the change in entropy of the concentrated photon beam then becomes

$$\Delta S = 2k_B \ln \left(1 + \frac{2v^2}{c^2} \frac{\xi}{N} \right). \tag{7}$$

Using the thermodynamic definition of entropy, $\delta Q / T$, rather than the statistical argument developed here, Eq. (7) can be equivalently recovered by assuming that the photon gas is an effective heat bath and δQ is the addition of two photons of energy hv.

III. BRIGHTNESS

Radiation will come into thermal equilibrium with the chromophore, provided that there is fast thermal equilibration between excited states [1,12]. As there are no first-order photon-photon interactions, photon beams cannot be in a true thermal equilibrium. Nevertheless, photon beams are well defined by thermodynamic parameters such as temperature, T, and chemical potential, μ [11]. The radiation emitted by a blackbody has zero chemical potential; however, quasiblackbody radiation, where radiation is emitted over a restricted range, may have a nonzero chemical potential. Planck derives the intensity of a monochromatic beam as

$$I = \frac{h\nu^3 n^2}{c^2} \frac{1}{e^{\frac{\mu - h\nu}{k_B T}} - 1}, \qquad (8)$$

which has units of energy per unit area, where k_B is the Boltzmann constant and T is the temperature of the medium in which emission from the chromophore takes place [Eq. (300) in Ref. [14]]. As radiation in thermodynamic equilibrium is isotropic and unpolarized, we can consider average chromophore absorption over 4π solid angle. Dividing Eq. (8) by the energy of the photon ($h\nu$), we determine the photon flux of a beam as

$$B = \frac{8\pi n^2 \nu^2}{c^2} \frac{1}{e^{\frac{\mu - h\nu}{k_B T}} - 1}. \qquad (9)$$

Equation (9) is often referred to as the brightness of the beam and has units of photons per second, per unit bandwidth, per 4π solid angle, per unit area [1,11,14,15]. For monochromatic brightness, we can write $\xi/N = 4\pi n^2/B$. Where the input beam has some frequency range, the treatment presented by Markvart may be used [12]. Brightness, like etendue, is conserved along the path of the beam in a perfectly transparent material. The transformation of one quasiequilibrium beam into another introduces irreversibility, bringing about entropy generation.

IV. CONCENTRATION LIMIT

The gain in entropy of the concentrated beam must be acquired from the free energy change associated with the photon-multiplicative process. For a traditional LSC with a chromophore of unity photoluminescence quantum efficiency, the concentration factor, C, is defined as the ratio of the brightnesses of the outgoing field, B_2, and the incoming field, B_1,

$$C \equiv \frac{B_2}{B_1} \leq \frac{\nu_2^2}{\nu_1^2} \exp\left(\frac{h(\nu_1 - \nu_2)}{k_B T}\right), \qquad (10)$$

where ν_1 and ν_2 are the frequencies of the input photon and output photon, respectively [1]. The concentration

limit of the PM-LSC can be determined from the second law of thermodynamics. Including the entropy source from the thermal loss, $h(\nu_1 - 2\nu_2)$, the second law can be written as

$$\underbrace{2k_B \ln\left(1 + \alpha \frac{\nu_2^2}{B_2}\right)}_{\Delta S_2} + \frac{h(\nu_1 - 2\nu_2)}{T} - \underbrace{k_B \ln\left(1 + \alpha \frac{\nu_1^2}{B_1}\right)}_{\Delta S_1} \geq 0, \qquad (11)$$

where $\alpha = 8\pi n^2/c^2$, and ΔS_1 and ΔS_2 correspond to the entropy changes in the incident photon field and the generated photon field, respectively. Assuming the LSC is operating in a normal terrestrial environment, where $\alpha \nu^2/B \gg 1$, the 1s in the logarithms can be ignored, and a concentration factor for PM-LSCs can be determined by rearranging Eq. (11):

$$\frac{B_2^2}{B_1} \leq \frac{8n^2\pi}{c^2} \frac{\nu_2^4}{\nu_1^2} \exp\left(\frac{h(\nu_1 - 2\nu_2)}{k_B T}\right). \qquad (12)$$

Hence, the concentration factor is given by

$$\frac{B_2}{B_1} \leq \sqrt{\frac{8n^2\pi}{B_1 c^2} \frac{\nu_2^4}{\nu_1^2} \exp\left(\frac{h(\nu_1 - 2\nu_2)}{k_B T}\right)}. \qquad (13)$$

Surprisingly, we find that for PM-LSCs the concentration limit is dependent on input brightness. Comparing the concentration limit of a PM-LSC, Eq. (13), to that of a traditional LSC, Eq. (10), we find similar design requirements but also some important distinctions [1].

In a traditional LSC, when the Stokes shift is zero ($\nu_1 = \nu_2$), there will be no associated thermal loss as $h(\nu_1 - \nu_2)/T = 0$, and the difference in the entropic terms associated with the addition and removal of the photon will equal, $\Delta S_2 - \Delta S_1 = 0$; thus, the LSC is unable to concentrate. However, the PM-LSC, particularly at low brightnesses, may concentrate, even if there is no thermal loss, i.e., $h(\nu_1 - 2\nu_2)/T = 0$. Even at the energy conservation limit, $\nu_1 = 2\nu_2$, there remains a source of entropy from the addition and removal of photons of different wavelengths, $\Delta S_2 - \Delta S_1$, which is sufficient to allow for concentration.

To increase the concentration limit of a PM-LSC, or to enable effective concentration at higher brightnesses, an additional thermal loss is required to satisfy the inequality in Eq. (13), analogous to the Stokes shift in the traditional LSC. As depicted in Figure 2, the concentration factor is exponentially dependent on the thermal loss in PM-LSCs. Figure 2 assumes that both the PM-LSC and LSC chromophore emissions are given by $h\nu_2 = 1.12$ eV, and thus, are optimized for the silicon photovoltaic band gap ($E_g = 1.12$ eV). Both the traditional LSC and the PM-LSC are assumed to have the same matrix medium, with a
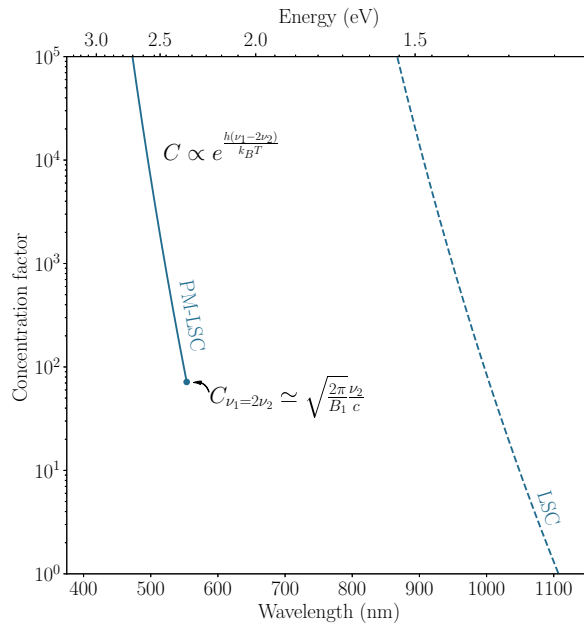
FIG. 2.   Maximum concentration factor as a function of chromophore absorption operating under terrestrial conditions. Dotted and solid lines give the maximum concentration factor, C, of the traditional LSC and PM-LSC, respectively, at room temperature ($T = 300$ K) with $n = 1$, when illuminated with light of brightness 10^9 photons per second per unit bandwidth per unit area per 4π solid angle. This brightness roughly approximates a broad chromophore absorption over the terrestrial solar spectrum (see Ref. [16] for further discussion). Emission for both the PM-LSC and the traditional LSC are fixed by $h\nu_2 = 1.12$ eV, to match the band gap of silicon photovoltaics. In the PM-LSC, the onset of the photon-multiplication process occurs at $\nu_1 = 2\nu_2$. Under normal terrestrial conditions, the PM-LSC may concentrate at $\nu_1 = 2\nu_2$, since the entropic change associated with the removal and addition of photons at different wavelengths ($\Delta S_2 - \Delta S_1$) is greater than zero. When absorbing higher-energy photons, $\nu_1 > 2\nu_2$, the maximum concentration factor increases as the thermal loss increases, analogous to the Stokes shift in the traditional LSC.

refractive index of $n = 1$. In the case of PM-LSCs, only photons with an energy of $h\nu_1 \geq 2.48$ eV may undergo a PM process to comply with the constraints imposed by the conservation of energy. The input brightness, B_1, is fixed at 10^9 photons per second per unit bandwidth per unit area per 4π solid angle. This brightness represents a broad absorption over the terrestrial solar spectrum for the PM-LSC, although there are difficulties in determining this value when approximating solar radiation over some narrow bandwidth (see Ref. [16]). Care must be taken when modeling much greater brightnesses, for example, where the input solar flux is concentrated before entry into the LSC or for extremely small band-gap materials, where Eq. (13) must be reformed, as $\alpha\nu^2/B \gg 1$ is no longer valid (see Ref. [16]).
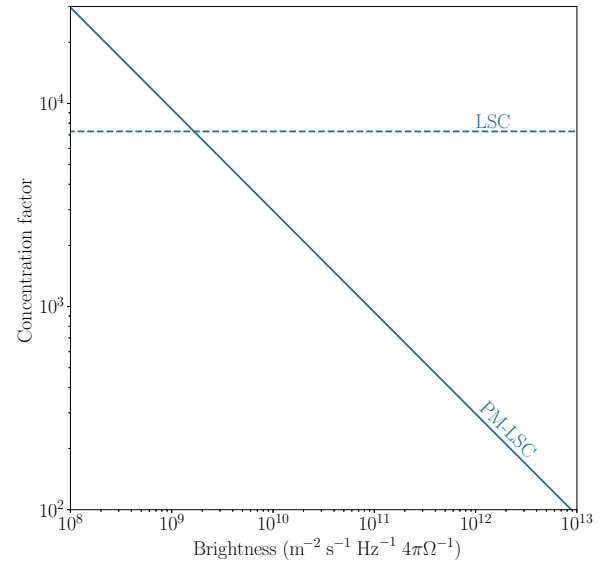

FIG. 3.   Maximum concentration factor at room temperature for a traditional LSC (dotted line) and a PM-LSC (solid line) as a function of incident brightness. Both the PM-LSC and traditional LSC concentration limits have an emission at $h\nu_2 = 1.12$ eV, which is optimized for silicon photovoltaics. Traditional LSC has a chromophore with a Stokes shift of 0.24 eV ($\lambda_1 = 912$ nm), which gives a brightness-independent maximum concentration factor, $C = 7280$. PM-LSC is assumed to be 200% efficient. PM-LSC has a thermal loss matching that of the traditional LSC, i.e. $h\nu_1 = 2 \times 1.12 + 0.24 = 2.48$ eV input, corresponding to monochromatic incident light of wavelength $\lambda_1 = 500$ nm.

We identify that, to achieve very high concentration factors, as for traditional LSCs, a PM-LSC design may also include thermal loss. Nevertheless, for some brightnesses, but equivalent thermal loss, the PM-LSC has a greater maximum concentration factor than that of the traditional LSC.

Figure 3 outlines the effect of input brightness on concentration factor. Here, again, the emission is optimized for a silicon photovoltaic band gap ($h\nu_2 = 1.12$ eV). In this case, however, the thermal loss is fixed at 0.24 eV for both the traditional LSC and the PM-LSC. The fixed thermal loss defines the monochromatic photon absorption at $\lambda_1 = 912$ nm in the traditional LSC and at $\lambda_1 = 500$ nm in the PM-LSC. For this specific thermal loss, only weak brightnesses allow for a maximum PM-LSC concentration factor greater than that of the traditional LSCs. Although the maximum concentration factor for PM-LSCs may increase more rapidly with increasing thermal loss relative to the traditional LSC, at very high brightness the PM-LSC cannot reach the same maximum concentration ratios as that of the traditional LSC.

Significant research efforts have been expended to improve the efficiencies and understand the mechanisms of photon-multiplier technologies [17,18]. As such, it is of general interest to determine how material design
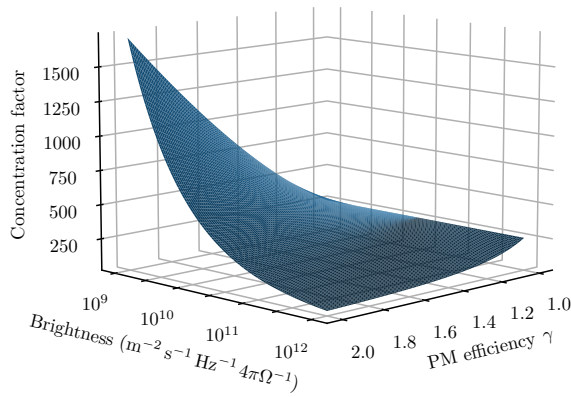
FIG. 4. Maximum concentration as function of PM efficiency and input brightness. Blue surface represents the maximum concentration factor for a PM-LSC with a variable PM efficiency, γ, under different incident brightness. γ varies from one, which would be the maximum efficiency of a traditional LSC, to two, the maximum efficiency of PM-LSCs considered here. Emission frequency for the PM-LSC is fixed at $h\nu_2 = 1.12$ eV, to match that of silicon photovoltaics. Incident illumination is described by a monochromatic beam with wavelength $h\nu_1 = 1.12\gamma + 0.15$ eV. Input brightness is plotted between 10^8 and 10^{12} photons per second per unit bandwidth per unit area per 4π solid angle.

improvements may impact on LSC uses and design. Figure 4 plots PM-LSC concentration as a function of γ, which is a measure of the PM system's efficiency between $1 \le \gamma \le 2$ (see Ref. [16] for the full expression). A maximally efficient traditional LSC chromophore will have $\gamma = 1$, meaning one photon absorbed will result in one photon being emitted by the chromophore, whereas a PM-LSC with 200% photon conversion efficiency has $\gamma = 2$. We note that, while the notion of a fractional γ is not physical in the single-photon limit, in the thermodynamic limit which we study, it is purely a ratio of underlying photon-yielding processes. For example, in organic semiconductors, the interplay between singlet fission or intersystem-crossing pathways for photoexcited singlets sets the effective γ of the system, with pure singlet fission yielding $\gamma = 2$ and pure intersystem crossing yielding $\gamma = 1$, assuming the triplets eventually yield luminescent species of interest [17].

Improvements in PM efficiency at low brightness would offer impressive concentration factors for PM-LSCs, suggesting that PM technologies may play an important role in low-brightness energy harvesting systems. At low brightness, even a small improvement in γ, from 1 to 1.2 would offer a twofold increase in the maximum concentration factor of PM-LSCs, implying that moving away from traditional LSCs to even a weakly efficient PM process yields gains in the concentration factor. For the highest brightnesses, however, a diminishing return on the investment of improving γ is made.

Taking the example of singlet fission photon-multiplier systems, Fig. 4 suggests that even a small improvement in singlet fission efficiency at low brightnesses could lead to impressive improvements in the maximum concentration factors of PM-LSCs. At high brightnesses, however, current demonstrations of singlet fission systems exhibit population-dependent annihilation effects, which would also diminish singlet fission efficiency [19].

Furthermore, this work suggests that exothermic singlet fission chromophores may lead to higher maximum concentration factors relative to endothermic singlet fission chromophores [17]. Without the inclusion of another heat source, endothermic singlet fission chromophores would act to reduce the entropic loss in Eq. (11), and hence, reduce the concentration limit.

Practical demonstrations of PM-LSCs utilize quantum cutting, where ytterbium-doped perovskite nanocrystals feature a photoluminescence quantum yield approaching 200% and virtually zero self-absorption loss [8,9]. These systems show great promise for PM-LSCs; however, the ytterbium-doped perovskite chromophores exhibit long-lived excited states on the order of milliseconds. These systems violate our assumption that the chromophore exhibits quick electronic recovery to a photon accepting state [20]. While these systems exhibit long-lived excited states, they will not reach the concentration limits described here.

Record demonstrations of traditional LSCs achieve concentration ratios on the order of 1–10 [21]. Although at high brightness the PM-LSC concentration limit is significantly below that of traditional LSCs, it is still on the order of 10^2–10^3. Analytical models and ray tracing simulations that explicitly include reabsorption effects better match concentration and optical efficiencies from practical demonstrations of LSCs [22]. In any case, without utilization of hot carrier solar cells coupled to LSCs, Auger recombination in standard photovoltaics will play a significant role at high photon flux, potentially hampering the potential gains of large concentration factors [23].

V. CONCLUSION

Considering the propagation and transformation of radiation in the thermodynamic limit, we obtain the entropy generation rate for a photon-multiplicative process. From the second law of thermodynamics, we obtain the concentration limit for an ideal PM-LSC. Unlike traditional LSCs, the maximum concentration in a PM-LSC is dependent on the brightness of the incident field. For very high concentration factors, particularly under bright conditions, the PM-LSC will require a large thermal loss, analogous to the Stokes shift in a traditional LSC. We find, at low brightness, the PM-LSC may exceed the concentration limit of traditional LSCs. Furthermore, at low brightness, the improvements required in the photon-multiplier efficiency

need only be small to have a dramatic impact on the concentration limit.

ACKNOWLEDGMENTS

[1] E. Yablonovitch, Thermodynamics of the fluorescent planar concentrator, J. Opt. Soc. Am. **70**, 1362 (1980).

[2] M. G. Debije and P. P. C. Verbunt, Thirty years of luminescent solar concentrator research: Solar energy for the built environment, Adv. Energy Mater. **2**, 12 (2011).

[3] U. W. P. U. Rau and T. Kirchartz, Thermodynamics of light management in photovoltaic devices, Phys. Rev. B **90**, 035211 (2014).

[4] A. Goetzberger, Fluorescent solar energy collectors: Operating conditions with diffuse light, Applied Physics **16**, 399 (1978).

[5] C. C. van Heerwaarden, W. B. Mol, M. Veerman, I. B. B. G. Heusinkveld, W. H. Knap, S. Kazadzis, N. Kouremeti, and S. Fiedler, Record high solar irradiance in Western Europe during first COVID-19 lockdown largely due to unusual weather, Commun. Earth Environ. **2**, 1 (2021).

[6] I. Papakonstantinou and C. Tummeltshammer, Fundamental limits of concentration in luminescent solar concentrators revised: The effect of reabsorption and nonunity quantum yield, Optica **2**, 841 (2015).

[7] J. S. Batchelder, A. H. Zewail, and T. Cole, Luminescent solar concentrators 2: Experimental and theoretical analysis of their possible efficiencies, Appl. Opt. **20**, 3733 (1981).

[8] T. D. X. Luo, Y. L. X. Liu, and K. Wu, Quantum-cutting luminescent solar concentrators using ytterbium-doped perovskite nanocrystals, Nano Lett. **19**, 338 (2018).

[9] T. A. Cohen, T. J. Milstein, D. M. Kroupa, J. D. MacKenzie, C. K. Luscombe, and D. R. Gamelin, Quantum-cutting perovskite nanocrystals for monolithic bilayer luminescent solar concentrators, J. Mater. Chem. A **7**, 9279 (2019).

[10] W. Shockley and H. J. Queisser, Detailed balance limit of efficiency of p-n junction solar cells, J. Appl. Phys. **32**, 510 (1961).

[11] L. Landau and E. M. Lifshitz, *Statistical Physics* (Pergamon Press, Oxford, 1980).

[12] T. Markvart, The thermodynamics of optical étendue, J. Opt. A: Pure Appl. Opt. **10**, 015008 (2007).

[13] T. Markvart, Solar cell as a heat engine: Energy-entropy analysis of photovoltaic conversion, Phys. Status Solidi (a) **205**, 2752 (2008).

[14] M. Planck, *The Theory of Heat Radiation* (Dover Publications, New York, 1991).

[15] R. T. Ross, Some thermodynamics of photochemical systems, J. Chem. Phys. **46**, 4590 (1967).

[16] See the Supplemental Material at http://link.aps.org/supplemental/10.1103/PRXEnergy.1.033001 for a discussion of terrestrial brightness, details of the entropy approximation used in the text, and the full form of the concentration ratio as a function of PM efficiency.

[17] A. Rao and R. H. Friend, Harnessing singlet exciton fission to break the Shockley–Queisser limit, Nat. Rev. Mater. **2**, 17063 (2017).

[18] T. J. Milstein, D. M. Kroupa, and D. R. Gamelin, Picosecond quantum cutting generates photoluminescence quantum yields over 100% in ytterbium-doped $CsPbCl_3$ nanocrystals, Nano Lett. **18**, 3792 (2018).

[19] J. Allardice, A. Thampi, S. Dowland, J. Xiao, G. Victor, Z. Zhang, P. Budden, A. J. Petty, N. J. L. K. Davies, N. C. Greenham, J. E. Anthony, and A. Rao, Engineering molecular ligand shells on quantum dots for quantitative harvesting of triplet excitons generated by singlet fission, J. Am. Chem. Soc. **141**, 12907 (2019).

[20] C. S. Erickson, M. J. Crane, T. J. Milstein, and D. R. Gamelin, Photoluminescence saturation in quantum-cutting Yb_3-doped $CsPb(Cl_{1-x}Br_x)_3$ perovskite nanocrystals: Implications for solar downconversion, J. Phys. Chem. C **123**, 12474 (2019).

[21] J. Roncali, Luminescent solar collectors: Quo vadis?, Adv. Energy Mater. **10**, 2001907 (2020).

[22] V. I. Klimov, T. A. Baker, J. Lim, K. A. Velizhanin, and H. McDaniel, Quality factor of luminescent solar concentrators and practical concentration limits attainable with semiconductor quantum dots, ACS Photonics **3**, 1138 (2016).

[23] J. Nelson, *The Physics of Solar Cells* (Imperial College Press, London, 2003).